Insufficient glucose supply is linked to hypothermia upon cold exposure in high-fat diet-fed mice lacking PEMT

Xia Gao,*,† Jelske N. van der Veen,*,† Carlos Fernandez-Patron,† Jean E. Vance,*,§ Dennis E. Vance,*,† and René L. Jacobs[1],*,**

Group on the Molecular and Cell Biology of Lipids* and Departments of Biochemistry,† Medicine,§ and Agricultural, Food, and Nutritional Science,** University of Alberta, Edmonton, Canada

Abstract **Mice that lack phosphatidylethanolamine *N*-methyltransferase (*Pemt*$^{-/-}$ mice) are protected from high-fat (HF) diet-induced obesity. HF-fed *Pemt*$^{-/-}$ mice show higher oxygen consumption and heat production, indicating that more energy might be utilized for thermogenesis and might account for the resistance to diet-induced weight gain. To test this hypothesis, HF-fed *Pemt*$^{-/-}$ and *Pemt*$^{+/+}$ mice were challenged with acute cold exposure at 4°C. Unexpectedly, HF-fed *Pemt*$^{-/-}$ mice developed hypothermia within 3 h of cold exposure. In contrast, chow-fed *Pemt*$^{-/-}$ mice, possessing similar body mass, maintained body temperature. Lack of PEMT did not impair the capacity for thermogenesis in skeletal muscle or brown adipose tissue. Plasma catecholamines were not altered by *Pemt* genotype, and stimulation of lipolysis was intact in brown and white adipose tissue of *Pemt*$^{-/-}$ mice. HF-fed *Pemt*$^{-/-}$ mice also developed higher systolic blood pressure, accompanied by reduced cardiac output. Choline supplementation reversed the cold-induced hypothermia in HF-fed *Pemt*$^{-/-}$ mice with no effect on blood pressure. Plasma glucose levels were ~50% lower in HF-fed *Pemt*$^{-/-}$ mice compared with *Pemt*$^{+/+}$ mice. Choline supplementation normalized plasma hypoglycemia and the expression of proteins involved in gluconeogenesis. We propose that cold-induced hypothermia in HF-fed *Pemt*$^{-/-}$ mice is linked to plasma hypoglycemia due to compromised hepatic glucose production.**—Gao, X., J. N. van der Veen, C. Fernandez-Patron, J. E. Vance, D. E. Vance, and R. L. Jacobs. **Insufficient glucose supply is linked to hypothermia upon cold exposure in high-fat diet-fed mice lacking PEMT. *J. Lipid Res.* 2015.** 56: **1701–1710.**

Supplementary key words adipose tissue • obesity • phosphatidylcholine • phosphatidylethanolamine • phosphatidylethanolamine *N*-methyltransferase • hypertension

Phosphatidylethanolamine *N*-methyltransferase (PEMT) catalyzes phosphatidylcholine (PC) biosynthesis via three sequential methylations of phosphatidylethanolamine (PE) (1). In the liver, PEMT contributes ~30% of hepatic PC production, whereas the remaining 70% of hepatic PC is synthesized via the CDP-choline pathway (2, 3). Normal levels of hepatic PC are required to maintain membrane integrity (4) and normal VLDL secretion (5–7). In mice, inhibition of either the CDP-choline pathway by liver-specific deletion of CTP:phosphocholine cytidylyltransferase (LCT)α or elimination of the PEMT pathway reduces hepatic PC content by ~30% and causes hepatic steatosis (8). The importance of the PEMT pathway has been highlighted in *Pemt*$^{-/-}$ mice fed either a choline-deficient diet (4) or a high-fat (HF) diet (9). When fed the HF diet for 10 weeks, *Pemt*$^{-/-}$ mice develop nonalcoholic steatohepatitis, but are protected against diet-induced obesity (DIO) and insulin resistance (9). HF-fed *Pemt*$^{-/-}$ mice also exhibit higher oxygen consumption than HF-fed *Pemt*$^{+/+}$ mice (9). *LCTα*$^{-/-}$ mice fed the HF diet also develop steatohepatitis (8–10), but are not protected from DIO (9). Thus, the resistance of *Pemt*$^{-/-}$ mice to DIO does not appear to rely primarily on decreased hepatic PC or impaired VLDL secretion (5, 6).

Increased oxygen consumption and heat production in HF-fed *Pemt*$^{-/-}$ mice (9) suggest thermogenesis in these mice might contribute to adipose hypotrophy in responding to the HF diet (9, 11). Cold exposure is widely used to

This research was supported by Canadian Institutes of Health Research Grants (MOP 5182 and MOP 133505). R.L.J. is a Canadian Institutes of Health Research New Investigator. X.G. was supported by a studentship from Alberta Innovates Health Solutions. The R.L.J. and D.E.V. laboratories are associated with the Alberta Diabetes Institute and the Alberta Mazankowski Heart Institute.

Manuscript received 20 March 2015 and in revised form 18 June 2015.

Published, JLR Papers in Press, June 25, 2015
DOI 10.1194/jlr.M059287

Abbreviations: ATGL, adipose TG lipase; BAT, brown adipose tissue; C/EBPβ, CCAAT/enhancer-binding protein β; DIO, diet-induced obesity; FABP4, fatty acid binding protein 4; HF, high-fat; HFCS, choline-supplemented high-fat; HSL, hormone-sensitive lipase; PC, phosphatidylcholine; PE, phosphatidylethanolamine; PEMT, phosphatidylethanolamine *N*-methyltransferase; PEPCK, phosphoenolpyruvate carboxykinase; PGC1α, PPARγ coactivator 1α; T3, triiodothyronine; T4, thyroxine; TGH, TG hydrolase; UCP, uncoupling protein; WAT, white adipose tissue.

[1]To whom correspondence should be addressed.
e-mail: rjacobs@ualberta.ca

The online version of this article (available at http://www.jlr.org) contains a supplement.

determine the capability for thermogenesis (12). Upon cold exposure, both skeletal muscle-mediated shivering thermogenesis and brown adipose tissue (BAT)-mediated nonshivering thermogenesis are activated to maintain the core body temperature (12). Intolerance to cold exposure might reflect inadequate heat production or a defective heart to accommodate the cold-activated catabolism (12).

In this study, we investigated the contribution of thermogenesis to the resistance of *Pemt*$^{-/-}$ mice to DIO. After consuming the HF diet for 2 weeks, *Pemt*$^{-/-}$ mice unexpectedly failed to maintain body temperature above 28°C during acute cold challenge. On the other hand, *Pemt*$^{-/-}$ mice that were fed a standard chow diet were able to maintain their body temperature over 33°C upon cold exposure. We explored the mechanisms underlying cold-induced hypothermia in HF-fed *Pemt*$^{-/-}$ mice. Dietary choline supplementation completely reversed the hypothermia in HF-fed *Pemt*$^{-/-}$ mice, with concomitant normalization of plasma glucose and markers of hepatic gluconeogenesis.

MATERIALS AND METHODS

Animal handling and diets

All procedures were approved by the University of Alberta's Institutional Animal Care Committee in accordance with guidelines of the Canadian Council on Animal Care. Male C57Bl/6 *Pemt*$^{+/+}$ and *Pemt*$^{-/-}$ mice were housed with free access to water and chow (LabDiet, #5001). *Pemt*$^{+/+}$ and *Pemt*$^{-/-}$ mice (8–9 weeks old) were fed a HF diet (60% calories from fat; Bio-Serv, #F3282) or choline-supplemented HF (HFCS) diet for 2 weeks. The HF diet contained 1.15 g choline per kg diet, and choline content was raised to 4 g choline per kg diet in the HFCS diet. Tissues were collected from mice that had either been fasted for 12 h or not fasted, as indicated. Blood was collected by cardiac puncture. Tissues were either used immediately for assessment of fatty acid oxidation or stored at −80°C.

The procedure for cold challenge was adapted from a previous study (13). Mice were fasted for 4 h then transferred to the cold room (4°C) with individual housing and no bedding, food, or water for up to 4 h. Rectal body temperature was determined hourly using a mouse rectal probe (model 4600 Precision thermometer). When the body temperature dropped below 28°C, the mice were removed from the cold room. Tissues were collected immediately after the cold exposure.

In vivo metabolic analysis

Metabolic measurements (heat production and beam breaks) were obtained using a comprehensive lab animal monitoring system (Columbus Instruments, Columbus, OH) as described (9). Mice were housed individually for 3 days before being placed in metabolic cages. Following an initial 24 h acclimatization period, measurements were taken every 13 min for 24 h.

Analytical procedures

Plasma TG and TG extracted from tissue (liver or interscapular BAT) homogenates were quantified using a commercially available kit from Roche Diagnostics. Plasma NEFAs and glucose were quantified using commercially available kits from Wako Chemicals GmbH and BioAssay Systems (14), respectively. Plasma thyroid hormones [triiodothyronine (T3) and thyroxine (T4)] were quantified by commercially available kits (Leinco Technologies, Inc.). Plasma epinephrine and norepinephrine were quantified with a commercially available 2-CAT (A-N) Research ELISA kit (Labor Diagnostika Nord). PC and PE extracted from BAT homogenates were quantified as previously described (15). Protein concentrations were determined by the Bradford assay (Bio-Rad). A portion of BAT was fixed in 10% buffered formalin and subjected to hematoxylin and eosin staining.

Fatty acid oxidation

The rate of fatty acid oxidation in interscapular BAT or gastrocnemius muscle was determined as described with minor modifications (11, 16). *Pemt*$^{+/+}$ and *Pemt*$^{-/-}$ mice were fed the HF diet for 2 weeks. After 12 h fasting, freshly isolated interscapular BAT or gastrocnemius muscle was gently homogenized in ice-cold buffer [10 mM Tris-HCl, 250 mM sucrose, 1 mM EDTA (pH 7.4)] followed by sonication for 10 s. After centrifugation at 500 *g* for 10 min at 4°C, the supernatant was collected and protein concentration was determined. The rate of [1-^{14}C]palmitate oxidation was determined over 1 h by capturing the amount of $^{14}CO_2$ released (complete oxidation) and by measuring the amount of ^{14}C-labeled acid-soluble metabolites (incomplete oxidation). Briefly, 1.5–2 mg BAT homogenate or 0.35–0.55 mg muscle homogenate protein (in 250 μl) was preincubated with the reaction mixture at 37°C for 5 min in a 25 ml glass vial. The glass vial was fitted with an Eppendorf tube containing Whatman filter paper (for injection of 150 μl of 1 M NaOH to capture the released CO_2) and was capped with a rubber stopper. The assay mixture contained 115 mM NaCl, 2.6 mM KCl, 10 mM Tris-HCl (pH 7.4), 1.2 mM KH_2PO_4, 10 mM $NaHCO_3$, 0.2 mM EDTA, 0.3% fatty acid-free BSA, 2 mM L-carnitine, 5 mM ATP, 0.5 mM malate, and 0.1 mM CoA. The reaction was initiated by injecting BSA-conjugated 0.2 mM palmitate (molar ratio 6:1 for palmitate:BSA), which contained 0.5 μCi/ml 1-^{14}C-palmitate, through the rubber stopper. After 1 h of incubation at 37°C, 300 μl of 3 M perchloric acid was injected to stop the reaction. The vials were left at room temperature for 2 h to capture the released CO_2. The radioactivity of CO_2 captured by the filter papers and the radioactivity in acid-soluble metabolites (in the supernatant) were measured by a scintillation counter.

Immunoblotting

Liver and interscapular BAT were homogenized in buffer [100 mM Tris-HCl, 150 mM sodium chloride, 1 mM EDTA, 1 mM DTT, and 0.1 mM PMSF (pH 7.4) containing a protease inhibitor cocktail. Gastrocnemius muscle was homogenized in buffer [50 mM Tris-HCl, 250 mM sucrose, 1 mM EDTA, 1 mM DTT, and 0.1 mM PMSF (pH 7.4)] containing a protease inhibitor cocktail. Proteins were transferred to a polyvinylidene difluoride membrane and the membrane was probed with primary antibodies against fatty acid binding protein 4 (FABP4) (Cell Signaling, #2120), PPARγ (Cell Signaling, #24443), CCAAT/enhancer-binding protein β (C/EBPβ) (Santa Cruz, sc150), PPARγ coactivator 1α (PGC1α) (Abcam, #ab54481), phosphoenolpyruvate carboxykinase (PEPCK) (Abcam, #ab70358), uncoupling protein (UCP)1 (Abcam, #ab10983), UCP2 (Abcam, #ab67241), UCP3 (Abcam, #ab3477), porin (VDAC; Abcam, #ab14734), complexes of the electron transport chain (Abcam, #ab110413), calnexin (Enzo Life Sciences, SPA-865), hormone-sensitive lipase (HSL) (Cell Signaling, #4107), phospho-HSL (Ser660; Cell Signaling, #4126), adipose TG lipase (ATGL) (Cell Signaling, #2138), TG hydrolase (TGH) (a gift from Dr. Richard Lehner), protein disulfide isomerase (PDI) (Enzo Life Sciences, SPA-890), or GAPDH (Abcam,

#ab8245). The immunoreactive bands were visualized by enhanced chemiluminescence (Amersham Biosciences) according to the manufacturer's instructions and protein levels were quantified using ImageJ software.

Real-time quantitative PCR and analysis of mitochondrial DNA content

RNA isolation, cDNA synthesis, and real-time quantitative PCR were performed as described previously (17). mRNA levels were normalized to β-actin mRNA; primer sequences are listed in supplementary Table 1. Mitochondrial DNA content was determined as described previously (17). Briefly, total DNA was extracted from livers using a DNEasy kit (Qiagen). The mitochondrial DNA copy number was calculated using real-time quantitative PCR by measuring mitochondrial DNA encoding mitochondrial NADH-ubiquinone oxidoreductase chain 1 versus a nuclear DNA encoding lipoprotein lipase.

Systolic blood pressure

Systolic blood pressure was measured indirectly using a commercially available computerized tail cuff plethysmography system (Kent Scientific Corporation, Torrington, CT) (18). Transthoracic echocardiography was performed as described (19) on mildly anesthetized mice using a Vevo 770 high-resolution imaging system equipped with a 30 MHz transducer (RMV-707b; VisualSonics, Toronto, Canada).

Statistical analysis

Data are expressed as mean ± SEM. Comparisons between two groups were performed using Student's *t*-test. For all other comparisons, a two-way ANOVA followed by a Bonferroni post hoc test of individual group differences was used. $P < 0.05$ was considered significant. Unless otherwise indicated, five to seven animals were used per group.

RESULTS

HF-fed *Pemt*$^{-/-}$ mice are hypothermic upon cold exposure

When fed the HF diet for 10 weeks, *Pemt*$^{-/-}$ mice exhibit higher oxygen consumption than *Pemt*$^{+/+}$ mice (9), indicating that higher energy expenditure for heat production might account for the resistance of HF-fed *Pemt*$^{-/-}$ mice to DIO. After 2 weeks of HF feeding, *Pemt*$^{-/-}$ mice showed higher heat production and physical activity, assessed by counts of beam breaks, than *Pemt*$^{+/+}$ mice in the dark cycle only, not the light cycle (**Fig. 1A, B**). The higher heat production and physical activity might account for the resistance to DIO in *Pemt*$^{-/-}$ mice. Thus, *Pemt*$^{-/-}$ and *Pemt*$^{+/+}$ mice were fed the HF diet for 2 weeks in the current study. *Pemt*$^{-/-}$ mice did not gain weight after HF feeding, compared with ~3.7 g body weight gain in *Pemt*$^{+/+}$ mice (Fig. 1C). To determine the capacity for thermogenesis, we exposed HF-fed *Pemt*$^{-/-}$ and *Pemt*$^{+/+}$ mice to an acute cold exposure. Unexpectedly, HF-fed *Pemt*$^{-/-}$ mice were unable to maintain their body temperature upon cold exposure, as the rectal body temperature rapidly (within 2 to 3 h) decreased below 28°C (Fig. 1D). In contrast, *Pemt*$^{+/+}$ mice maintained their body temperature above 30°C throughout 4 h cold exposure (Fig. 1D).

The difference in body weight between *Pemt*$^{-/-}$ and *Pemt*$^{+/+}$ mice might have caused the cold-induced hypothermia in HF-fed *Pemt*$^{-/-}$ mice. However, chow-fed *Pemt*$^{-/-}$ and *Pemt*$^{+/+}$ mice, who had negligible body weight differences (**Fig. 2A**), maintained their body temperature above 33°C for up to 4 h of cold exposure (Fig. 2B). Thus, upon cold exposure, HF-fed *Pemt*$^{-/-}$ mice develop hypothermia, which is not caused by lower body weight.

PEMT deficiency does not impair oxidative capacity of skeletal muscle

Cold exposure of mice stimulates shivering thermogenesis, which is mainly mediated by skeletal muscle, to maintain their core body temperature (12). We thus examined the thermogenic capacity of skeletal muscle, freshly dissected from *Pemt*$^{+/+}$ and *Pemt*$^{-/-}$ mice fed the HF diet for 2 weeks, without being exposed to cold. The rate of incomplete fatty acid oxidation, as measured by ^{14}C incorporation into acid soluble metabolites in gastrocnemius muscle from *Pemt*$^{-/-}$ mice, was not different from that in *Pemt*$^{+/+}$ mice, whereas the rate of complete fatty acid oxidation, as measured by $^{14}CO_2$ generation, was higher in *Pemt*$^{-/-}$ mice than in *Pemt*$^{+/+}$ mice (**Fig. 3A**). The amounts of mitochondrial marker protein VDAC and electron transport chain proteins (complexes I to V) were the same in *Pemt*$^{-/-}$ and *Pemt*$^{+/+}$ mice (Fig. 3B). Furthermore, levels of UCP2 and UCP3 in *Pemt*$^{-/-}$ mice were comparable to those in *Pemt*$^{+/+}$ mice (Fig. 3B). Thus, *Pemt*$^{-/-}$ mice seem to have intact oxidative capacity in skeletal muscle.

PEMT deficiency does not alter thermogenic features of BAT

BAT-mediated thermogenesis is promoted by cold exposure. We considered the possibility that defective BAT-mediated thermogenesis contributed to hypothermia in HF-fed *Pemt*$^{-/-}$ mice. Thus, we examined the thermogenic capacity in BAT. PEMT protein (supplementary Fig. 1A) and its enzymatic activity (data not shown) were undetectable in BAT. When fed a standard chow diet, BAT from *Pemt*$^{-/-}$ mice contained the same amount of PC (61.05 ± 2.46 nmol/mg protein vs. 61.36 ± 2.31 nmol/mg protein in *Pemt*$^{+/+}$ mice) and TG (1.89 ± 0.15 μmol/mg protein vs. 2.11 ± 0.11 nmol/mg protein in *Pemt*$^{+/+}$ mice) as *Pemt*$^{+/+}$ mice. When the mice were fed the HF diet for 2 weeks, the mass of BAT was the same between genotypes (**Fig. 4A**). The levels of PC and PE, and the PC/PE ratio, in BAT were not different between *Pemt*$^{-/-}$ and *Pemt*$^{+/+}$ mice (supplementary Fig. 1B). However, BAT from *Pemt*$^{-/-}$ mice contained slightly less TG than did BAT from *Pemt*$^{+/+}$ mice under nonfasting conditions (supplementary Fig. 1C). Fasting greatly reduced TG storage to a similar extent in both genotypes, as shown in histological analysis and biochemical measurement (Fig. 4B, supplementary Fig. 1C), indicating that fasting-induced lipolysis was intact in BAT from *Pemt*$^{-/-}$ mice.

Lack of PEMT did not significantly impair adipocyte differentiation in BAT. The protein levels of adipocyte differentiation markers PPARγ and FABP4 were the same in HF-fed *Pemt*$^{-/-}$ mice and *Pemt*$^{+/+}$ mice, but the amount of

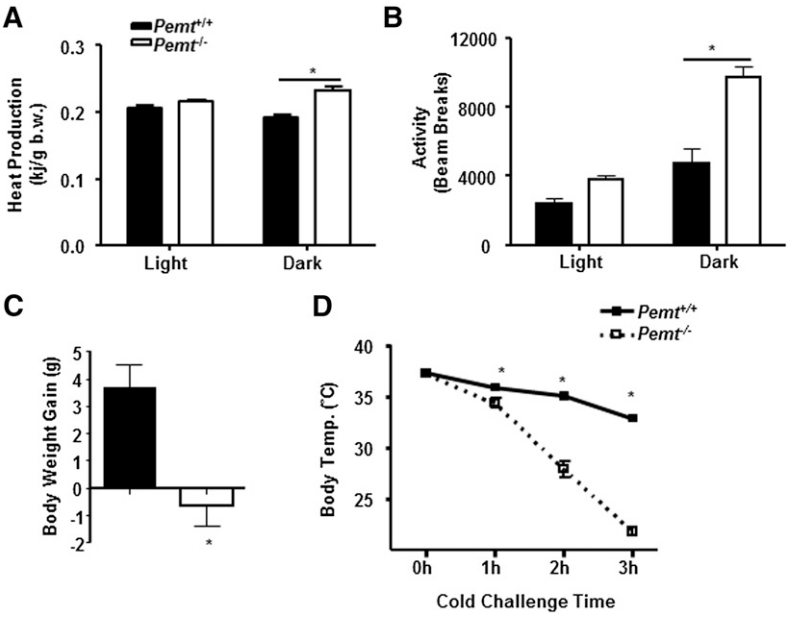

Fig. 1. HF-fed *Pemt*$^{-/-}$ mice are hypothermic upon cold exposure. *Pemt*$^{+/+}$ and *Pemt*$^{-/-}$ mice (8–9 weeks old) were fed the HF diet for 2 weeks. A, B: Mice were housed individually for 3 days then placed in metabolic cages for metabolic measurements throughout the light and dark cycles. Heat production (A) and physical activity (B) accessed by beam breaks. b.w., body weight. C: HF-induced body weight gain. D: Rectal temperature (Temp.) during cold challenge. Mice were fasted for 4 h then placed at 4°C without bedding, food, or water. All data are from five to six mice of each genotype; *$P < 0.05$ by Student *t*-test for *Pemt*$^{+/+}$ versus *Pemt*$^{-/-}$.

C/EBPβ protein was reduced by 56% by PEMT deficiency (Fig. 4C). However, in mice fed a standard chow diet, the protein levels of FABP4 and C/EBPβ were not different between *Pemt* genotypes (data not shown). Thus, PEMT deficiency does not impair the differentiation of brown adipocytes. The reduced amount of C/EBPβ protein in HF-fed *Pemt*$^{-/-}$ mice suggests that lipogenesis might be reduced, which might account for the minor reduction of TG in BAT under nonfasting conditions (supplementary Fig. 1C).

We next explored the thermogenic capacity of BAT. The protein levels of UCP1 and PGC1α, a key regulator of oxidative metabolism and UCP1-mediated thermogenesis in BAT (20), were not different between genotypes (Fig. 4D). Moreover, amounts of the mitochondrial marker protein VDAC and mitochondrial electron transport chain proteins (complexes I to V) were the same in BAT from *Pemt*$^{-/-}$ and *Pemt*$^{+/+}$ mice (Fig. 4D). PEMT deficiency did not alter mitochondrial number either (Fig. 4E). Furthermore, the rates of complete fatty acid oxidation (measured as the amount of released $^{14}CO_2$) and incomplete fatty acid oxidation (measured as the amount of ^{14}C-labeled acid-soluble metabolites) in BAT from *Pemt*$^{-/-}$ mice were similar to those in *Pemt*$^{+/+}$ mice (Fig. 4F). Overall, BAT of HF-fed *Pemt*$^{-/-}$ mice and *Pemt*$^{+/+}$ mice exhibits comparable thermogenic features.

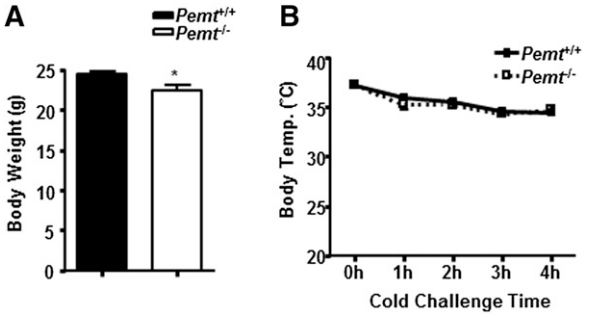

Fig. 2. Chow-fed *Pemt*$^{-/-}$ mice do not develop hypothermia upon cold exposure. *Pemt*$^{+/+}$ and *Pemt*$^{-/-}$ mice (10–11 weeks old) were fed a standard chow diet. Body weight (A) and rectal temperature (Temp.) (B) during cold challenge. Mice were fasted for 4 h then placed at 4°C without bedding, food, or water. All data are from six to seven mice of each group; *$P < 0.05$ by Student *t*-test for *Pemt*$^{+/+}$ versus *Pemt*$^{-/-}$.

Cold-stimulated adrenergic activation of lipolysis in adipose tissues is intact in *Pemt*$^{-/-}$ mice

Cold activates the sympathetic nervous system, particularly via the release of norepinephrine, which stimulates lipolysis in white adipose tissue (WAT) to provide substrates for thermogenesis to maintain core body temperature (21). However, after cold exposure, plasma levels of epinephrine and norepinephrine were not lower in *Pemt*$^{-/-}$ mice than in *Pemt*$^{+/+}$ mice (**Fig. 5A**). The lipases HSL and ATGL contribute over 95% of lipolytic activity in adipose tissue (22). Following cold exposure, WAT from *Pemt*$^{-/-}$ mice contained 1.7-fold more phospho-HSL and the same amount of total HSL (Fig. 5B) as did *Pemt*$^{+/+}$ mice. Thus, the ratio of phospho-HSL/HSL in WAT of *Pemt*$^{-/-}$ mice was higher than in *Pemt*$^{+/+}$ mice, indicating more activated HSL in *Pemt*$^{-/-}$ mice compared with *Pemt*$^{+/+}$ mice. The amounts of ATGL protein and another lipolytic enzyme, TGH, in WAT from *Pemt*$^{-/-}$ mice were also higher than in *Pemt*$^{+/+}$ mice (Fig. 5B). Consequently, the levels of fatty acids in plasma were elevated by cold exposure in both *Pemt*$^{-/-}$ and *Pemt*$^{+/+}$ mice to a similar level (Fig. 5C), compared with mice not exposed to cold (11). Thus, the exacerbation of cold-induced hypothermia in *Pemt*$^{-/-}$ mice does not appear to be caused by inefficient lipolysis in WAT.

Following cold exposure, the protein levels of phospho-HSL, total-HSL, and ATGL in BAT from *Pemt*$^{-/-}$ mice were indistinguishable from those in *Pemt*$^{+/+}$ mice (supplementary Fig. 2A). In contrast, the amount of TGH protein was lower in BAT from *Pemt*$^{-/-}$ mice than from *Pemt*$^{+/+}$

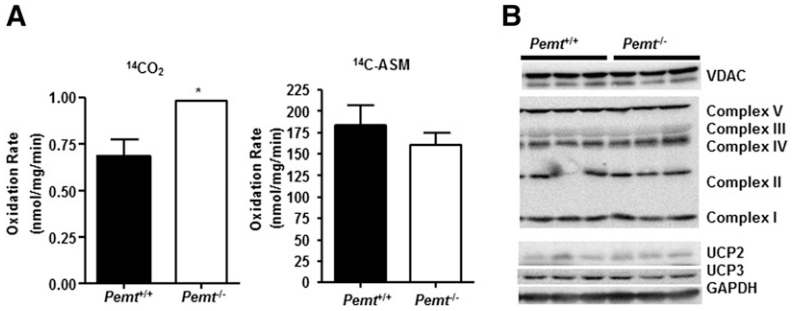

Fig. 3. Oxidative capacity of skeletal muscle from HF-fed *Pemt*$^{-/-}$ mice and *Pemt*$^{+/+}$ mice. *Pemt*$^{+/+}$ and *Pemt*$^{-/-}$ mice (8–9 weeks old) were fed the HF diet for 2 weeks. Gastrocnemius muscle was collected from mice after an overnight fast, without being exposed to cold. A: The rate of complete ($^{14}CO_2$) and incomplete (^{14}C-ASM) fatty acid oxidation was measured in skeletal muscle homogenates. Data are from five to seven mice of each group; $^*P < 0.05$ by Student *t*-test for *Pemt*$^{+/+}$ versus *Pemt*$^{-/-}$. B: Immunoblots of VDAC, electron transport chain complexes I to V, UCP2, UCP3, and the loading control, GAPDH. Data are from three mice of each group.

mice (supplementary Fig. 2A). Cold exposure reduced the amount of TG in BAT from mice of both genotypes compared with BAT collected from nonfasted mice (supplementary Figs. 1C, 2B). After cold exposure, however, BAT from *Pemt*$^{-/-}$ mice contained 49% less TG than did BAT from *Pemt*$^{+/+}$ mice (supplementary Fig. 2B). In addition, amounts of the mitochondrial protein VDAC and mitochondrial number (supplementary Fig. 2C, D) were not influenced by *Pemt* genotype. The level of PGC1α in BAT from *Pemt*$^{-/-}$ mice was slightly lower than that in *Pemt*$^{+/+}$ mice, whereas the amount of UCP1 protein was 2-fold higher in the *Pemt*$^{-/-}$ mice (supplementary Fig. 2C). Moreover, the amounts of mitochondrial electron transport chain proteins were equivalent in BAT from *Pemt*$^{+/+}$ and *Pemt*$^{-/-}$ mice, except for a slightly higher amount of complex V in the *Pemt*$^{-/-}$ mice (supplementary Fig. 2C). Furthermore, compared with *Pemt*$^{+/+}$ mice, BAT from *Pemt*$^{-/-}$ mice contained higher levels of mRNAs encoding proteins involved in fatty acid oxidation, such as carnitine palmitoyltransferase 1α (CPT1α) and long-chain acyl-CoA

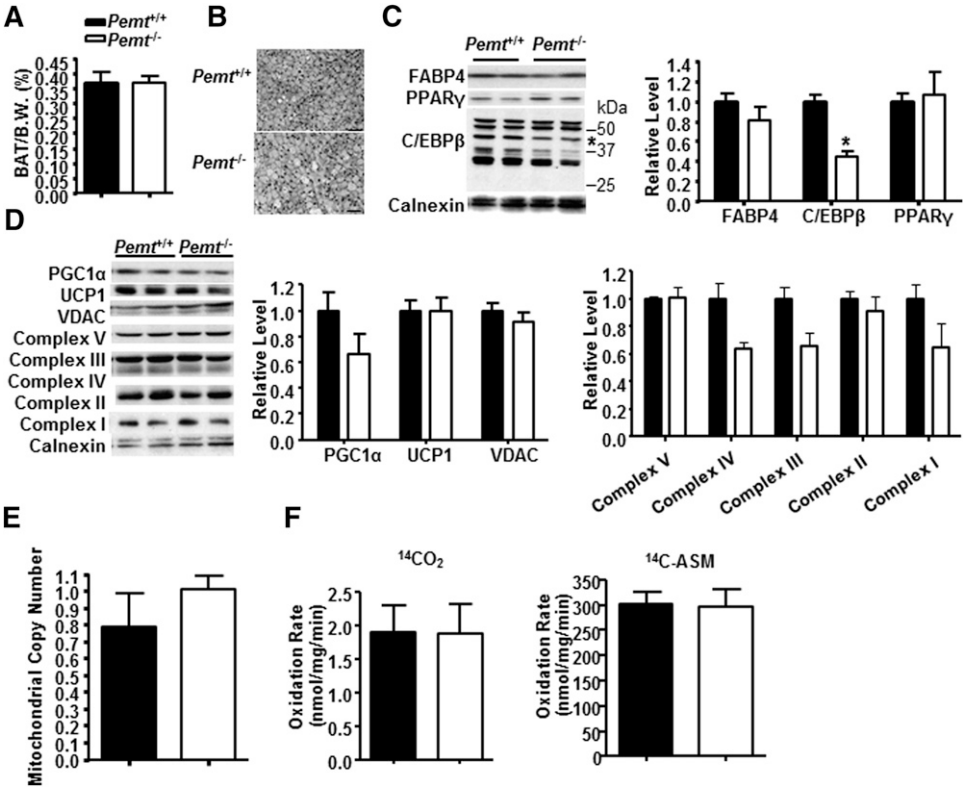

Fig. 4. Comparable oxidative capacity in BAT from HF-fed *Pemt*$^{-/-}$ mice and *Pemt*$^{+/+}$ mice. *Pemt*$^{+/+}$ and *Pemt*$^{-/-}$ mice (8–9 weeks old) were fed the HF diet for 2 weeks. BAT was collected from mice that had been fasted overnight. A: Weight of BAT as percent body weight (B.W.). B: Hematoxylin and eosin staining of BAT; bar: 50 μm. C: Representative immunoblots of C/EBPβ (indicated by the star), FABP4, PPARγ, and their densitometric analysis relative to the loading control, calnexin. D: Representative immunoblots of PGC1α, UCP1, VDAC, and electron transport chain complexes I to V and their densitometric analysis relative to the loading control calnexin. E: Mitochondrial copy number was assessed as the ratio of mitochondrial NADH-ubiquinone oxidoreductase chain 1 (*Nd1*) versus a nuclear DNA encoding lipoprotein lipase (*Lpl*). F: The rate of complete ($^{14}CO_2$) and incomplete (^{14}C-ASM) fatty acid oxidation in BAT homogenates. All data are from five to seven mice of each group; $^*P < 0.05$ by Student *t*-test for *Pemt*$^{+/+}$ versus *Pemt*$^{-/-}$.

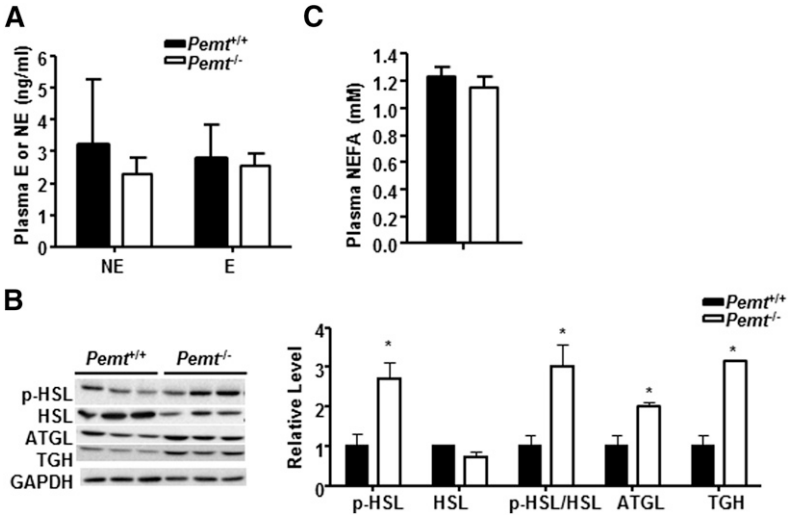

Fig. 5. Capacity for cold-stimulated TG lipolysis in WAT. *Pemt*$^{+/+}$ and *Pemt*$^{-/-}$ mice (8–9 weeks old) were fed the HF diet for 2 weeks followed by a 4 h fast and cold exposure. A: Plasma levels of epinephrine (E) and norepinephrine (NE). B: Representative immunoblots of lipolytic enzymes: phospho-HSL (p-HSL), total-HSL (HSL), ATGL, TGH, and their densitometric analysis relative to the loading control GAPDH. C: Levels of plasma NEFAs. All data are from five to seven mice of each group; *$P < 0.05$ by Student *t*-test for *Pemt*$^{+/+}$ versus *Pemt*$^{-/-}$.

dehydrogenase (LCAD) (supplementary Fig. 2E). The amounts of mRNAs encoding medium-chain acyl-CoA dehydrogenase (MCAD) and pyruvate dehydrogenase kinase isozyme 4 (PDK4) were not different between genotypes (supplementary Fig. 2E). Thus, in *Pemt*$^{-/-}$ mice, the HF-induced hypothermia is not the result of impaired adrenergic activation of BAT.

Systolic hypertension and reduced cardiac output in HF-fed *Pemt*$^{-/-}$ mice

Cold exposure stimulates cardiac output and blood flow to BAT (23, 24). To determine whether the cold-induced hypothermia in HF-fed *Pemt*$^{-/-}$ mice could be attributed to an insufficient circulatory system, we measured systolic blood pressure in *Pemt*$^{+/+}$ and *Pemt*$^{-/-}$ mice with a computerized tail cuff plethysmography system (18). Systolic blood pressure in HF-fed *Pemt*$^{-/-}$ mice was 20% higher than in HF-fed *Pemt*$^{+/+}$ mice (**Fig. 6A**), but heart weight was the same in mice of both genotypes (Fig. 6B). Cardiac function of these mice was evaluated by echocardiography (supplementary Methods). In *Pemt*$^{-/-}$ mice, the ejection fraction, fraction shortening, and cardiac output were 17, 21, and 25% lower than in *Pemt*$^{+/+}$ mice (Fig. 6C). However, heart rate was not altered by *Pemt* genotype (supplementary Table 2). Furthermore, *Pemt*$^{-/-}$ mice exhibited lower mitral early and late ventricular filling velocities, suggesting that *Pemt*$^{-/-}$ mice had diastolic dysfunction and longer left ventricle isovolumic contraction time than *Pemt*$^{+/+}$ mice (supplementary Table 2). These data indicate that the HF-induced hypothermia in *Pemt*$^{-/-}$ mice might be linked to hypertension, accompanied by reduced cardiac output.

Choline supplementation prevents cold-induced hypothermia in HF-fed *Pemt*$^{-/-}$ mice

Our previous studies have revealed that *Pemt*$^{-/-}$ mice are resistant to DIO due to choline insufficiency (9). HF-induced steatohepatitis in *Pemt*$^{-/-}$ mice is also improved by increased dietary choline (10). To determine whether the hypothermia in HF-fed *Pemt*$^{-/-}$ mice was also related to choline insufficiency, we increased the amount of choline to 4 g/kg diet in the HF diet that we fed for 2 weeks. Remarkably, choline supplementation completely prevented the hypothermia in *Pemt*$^{-/-}$ mice (**Fig. 7A**). All *Pemt*$^{+/+}$ mice that were fed either the HF or the HFCS diet maintained their body temperature upon cold exposure. Moreover, the HFCS diet increased body weight in *Pemt*$^{-/-}$ mice (Fig. 7B) without increasing the weight of BAT or

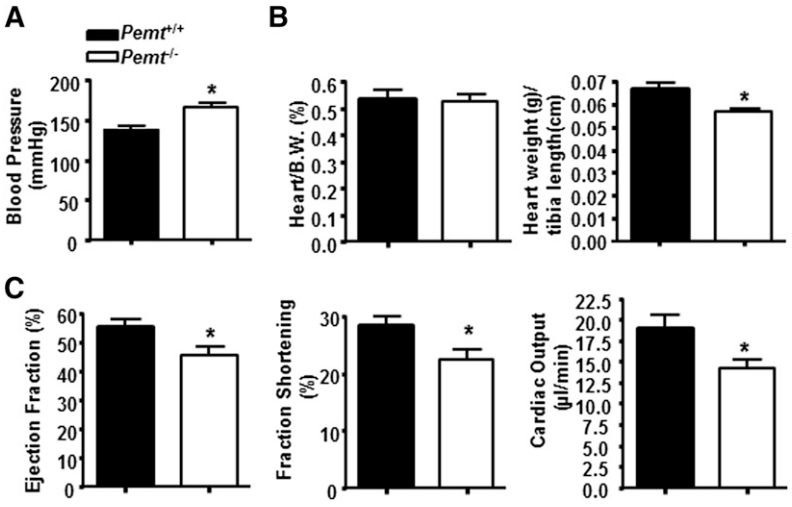

Fig. 6. Blood pressure and cardiac output in HF-fed *Pemt*$^{+/+}$ and *Pemt*$^{-/-}$ mice. The mice were fed the HF diet for 2 weeks. A: Systolic blood pressure was measured by a computerized tail cuff plethysmography system. B: Heart mass as percent of body weight (B.W.) and as percent of tibia length (in centimeters). C: In vivo cardiac function was determined by echocardiography: left ventricle ejection fraction, fraction shortening, and cardiac output. All data are from five to six mice of each genotype; *$P < 0.05$ by Student *t*-test for *Pemt*$^{+/+}$ versus *Pemt*$^{-/-}$.

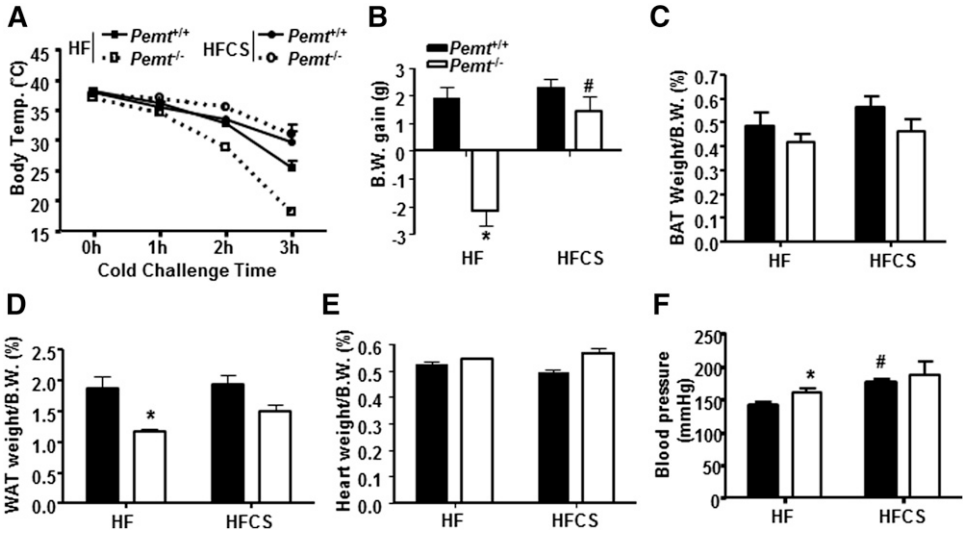

Fig. 7. Choline supplementation prevents hypothermia in HF-fed $Pemt^{-/-}$ mice. $Pemt^{+/+}$ and $Pemt^{-/-}$ mice were fed the HF or HFCS diet for 2 weeks followed by a 4 h fast and cold exposure. A: Rectal temperature during cold challenge. B: Body weight (B.W.) gain over the 2 weeks of feeding. C: BAT weight as percent of B.W. D: WAT weight as percent of B.W. E: Heart weight as percent of B.W. F: Systolic blood pressure in mice fed the HF or HFCS diet for 2 weeks without fasting or cold exposure. All data are from four to seven mice of each group; $^{*}P < 0.05$ by two-way ANOVA for $Pemt^{+/+}$ versus $Pemt^{-/-}$; $^{\#}P < 0.05$ by two-way ANOVA for the HF diet versus the HFCS diet for the same genotype.

WAT (Fig. 7C, D). In $Pemt^{+/+}$ mice, the HFCS diet did not alter body weight gain or the mass of BAT or WAT (Fig. 7C, D). The heart weight was not different among the four groups of mice (Fig. 7E). Moreover, the HFCS diet increased blood pressure in $Pemt^{+/+}$ mice, but not in $Pemt^{-/-}$ mice (Fig. 7G), implying that the higher blood pressure was not a causative factor for the hypothermia. These data demonstrate that choline supplementation prevents cold-induced hypothermia in HF-fed $Pemt^{-/-}$ mice, whereas the higher blood pressure in the HF-fed $Pemt^{-/-}$ mice does not contribute to this process.

Because thyroid hormones are also regulators of thermogenesis (21), we measured plasma levels of thyroid hormones in $Pemt^{+/+}$ and $Pemt^{-/-}$ mice fed the HF diet or the HFCS diet. In comparison to HF-fed $Pemt^{+/+}$ mice, the level of plasma T4 was 38% higher in HF-fed $Pemt^{-/-}$ mice, and this increase was prevented by choline supplementation (supplementary Fig. 3A). However, the level of plasma T3, the more active form of thyroid hormone, was 69% lower in $Pemt^{-/-}$ mice than in $Pemt^{+/+}$ mice, and this difference was not eliminated by choline supplementation (supplementary Fig. 3A). Thus, cold-induced hypothermia in HF-fed $Pemt^{-/-}$ mice is unlikely to be due to insufficient thyroid hormone T3.

Choline supplementation normalizes plasma glucose in HF-fed $Pemt^{-/-}$ mice

Surprisingly, in $Pemt^{-/-}$ mice fed the HF diet for 2 weeks, the cold-induced weight loss was less than in $Pemt^{+/+}$ mice, but this difference was completely normalized by choline supplementation (**Fig. 8A**). However, a 4 h fasting period prior to the cold exposure led to the same amount of weight loss in the four groups of mice (supplementary Fig. 3B). To gain further insight into the mechanism underlying the cold sensitivity of $Pemt^{-/-}$ mice, we investigated the energy supply in plasma after cold exposure of the mice. As shown in Fig. 8B, the amount of NEFAs in plasma of HF-fed $Pemt^{-/-}$ mice was the same as in $Pemt^{+/+}$ mice, and was not changed by choline supplementation (Fig. 8B). Plasma TG was not different between cold-exposed HF-fed $Pemt^{-/-}$ mice and $Pemt^{+/+}$ mice (Fig. 8C). The HFCS diet increased the amount of plasma TG in $Pemt^{+/+}$ mice, but not in $Pemt^{-/-}$ mice (Fig. 8C). However, the level of plasma glucose in HF-fed $Pemt^{-/-}$ mice was 49% lower than in $Pemt^{+/+}$ mice (**Fig. 9A**). Although the HFCS diet did not alter plasma glucose levels in $Pemt^{+/+}$ mice, plasma glucose was increased by 180% in the $Pemt^{-/-}$ mice (Fig. 9A). Thus, these data suggest that reduced plasma glucose, rather than TG or fatty acids, contributes to the cold-induced hypothermia in HF-fed $Pemt^{-/-}$ mice.

The liver is the major site of glucose production (25). HF-fed $Pemt^{-/-}$ mice show an attenuated hepatic gluconeogenesis and reduced hepatic glycogen (10, 26). To determine whether differences in plasma glucose in $Pemt^{+/+}$ and $Pemt^{-/-}$ mice were due to hepatic gluconeogenesis, we measured the amounts of a key enzyme in hepatic gluconeogenesis, PEPCK, and its transcription regulator, PGC1α (Fig. 9B, C). Compared with livers of HF-fed $Pemt^{+/+}$ mice, livers of HF-fed $Pemt^{-/-}$ mice contained 46% less PEPCK protein. Choline supplementation completely restored the amount of this protein to that in HF-fed $Pemt^{+/+}$ mice. Similarly, the amount of PGC1α in the livers of $Pemt^{-/-}$ mice was 68% lower than in HF-fed $Pemt^{+/+}$ mice, and the HFCS diet modestly increased the level of PGC1α in $Pemt^{-/-}$ mice. Moreover, the HFCS diet increased the lower level of TG in BAT from $Pemt^{-/-}$ mice to that in $Pemt^{+/+}$ mice (supplementary Fig. 4). Together, it

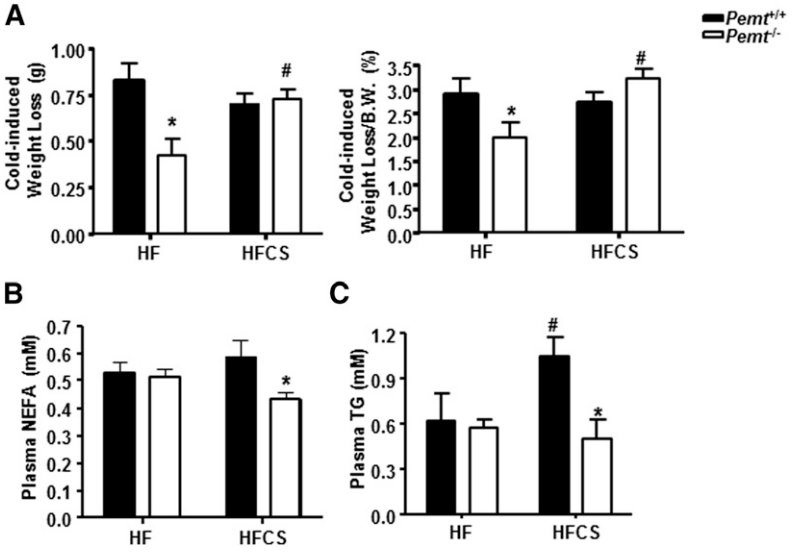

Fig. 8. Choline prevents cold-induced weight loss and normalizes plasma glucose in HF-fed *Pemt*$^{-/-}$ mice. *Pemt*$^{+/+}$ and *Pemt*$^{-/-}$ mice were fed the HF diet or HFCS diet for 2 weeks, followed by a 4 h fast and cold exposure. A: Cold-induced weight loss in grams (left panel) and as percent of body weight (B.W.) (right panel). B: Plasma NEFAs. C: Plasma TG. All data are from four to seven mice of each group; $^{*}P < 0.05$ by two-way ANOVA for *Pemt*$^{+/+}$ versus *Pemt*$^{-/-}$; $^{\#}P < 0.05$ by two-way ANOVA for HF diet versus HFCS diet for the same genotype.

appears that impaired hepatic gluconeogenesis is associated with cold-induced hypothermia in HF-fed *Pemt*$^{-/-}$ mice.

DISCUSSION

We report the unexpected finding that HF-fed *Pemt*$^{-/-}$ mice develop hypothermia upon cold exposure. However, HF-fed *Pemt*$^{-/-}$ mice show intact thermogenic features in skeletal muscle and in BAT, where PEMT activity is undetectable. Moreover, HF-fed *Pemt*$^{-/-}$ mice exhibit systolic hypertension and reduced cardiac output. This cold-induced hypothermia, but not the hypertension, in HF-fed *Pemt*$^{-/-}$ mice is prevented by dietary choline supplementation. Importantly, plasma glucose levels are ~50% lower in HF-fed *Pemt*$^{-/-}$ mice than in HF-fed *Pemt*$^{+/+}$ mice. Choline supplementation normalizes the plasma glucose and raises the expression of hepatic gluconeogenesis-related genes. Together, our results strongly support a link between insufficient plasma glucose supply and cold-induced thermogenesis in HF-fed *Pemt*$^{-/-}$ mice.

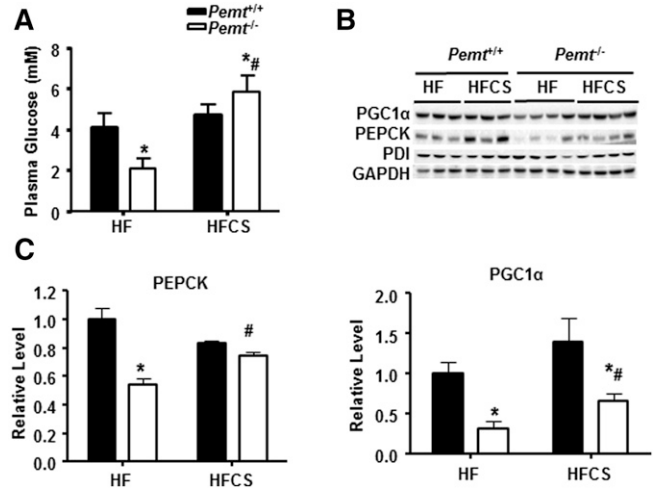

Fig. 9. Choline normalizes reduced expression of hepatic gluconeogenesis related genes in HF-fed *Pemt*$^{-/-}$ mice. *Pemt*$^{+/+}$ and *Pemt*$^{-/-}$ mice were fed the HF diet or HFCS diet for 2 weeks, followed by a 4 h fast and cold exposure. A: Plasma glucose. B: Representative immunoblots of PEPCK, PGC1α, protein disulfide isomerase (PDI), and GAPDH. C: Densitometric analysis of amounts of proteins in (B), which were normalized to the amount of GAPDH. All data are from four to seven mice of each group; $^{*}P < 0.05$ by two-way ANOVA for *Pemt*$^{+/+}$ versus *Pemt*$^{-/-}$; $^{\#}P < 0.05$ by two-way ANOVA for HF diet versus HFCS diet for the same genotype.

As was the case for mice fed the HF diet for 10 weeks (9), *Pemt*$^{-/-}$ mice fed the HF diet for only 2 weeks show HF-induced phenotypes: steatohepatitis and resistance to diet-induced adipose hypertrophy (10, 11). Moreover, *Pemt*$^{-/-}$ mice fed the HF diet for 2 weeks also have elevated heat production and physical activity compared with HF-fed *Pemt*$^{-/-}$ mice, but only in the dark cycle (Fig. 1A, B). All these data imply that HF-fed *Pemt*$^{-/-}$ mice expend more energy than *Pemt*$^{+/+}$ mice to maintain body temperature under normal housing conditions (at 22–25°C), when thermogenesis is anticipated to be enhanced compared with that of mice housed under thermoneutral conditions at ~30°C (12). The increased energy utilized for thermogenesis at 22–25°C could account for the resistance of HF-fed *Pemt*$^{-/-}$ mice to DIO. Thus, it is quite surprising that HF-fed *Pemt*$^{-/-}$ mice become hypothermic upon cold exposure (Fig. 1E). Even though HF-fed *Pemt*$^{-/-}$ mice contained less WAT mass (11) than HF-fed *Pemt*$^{+/+}$ mice, our data indicate that the cold-induced hypothermia of *Pemt*$^{-/-}$ mice is not due to reduced insulation caused by lower body fat mass. Indeed, chow-fed *Pemt*$^{-/-}$ mice have the same amount of body mass and contain the same WAT mass as HF-fed *Pemt*$^{-/-}$ mice (11), but are not cold sensitive (Fig. 2B).

Cold exposure activates the sympathetic nervous system and stimulates energy utilization for thermogenesis, particularly in BAT, to maintain core body temperature (21). Cold-induced sympathetic activity stimulates β-adrenergic

receptors on brown adipocytes for promotion of lipolysis for UCP1-mediated thermogenesis. Acute cold exposure also stimulates shivering thermogenesis in skeletal muscle to defend body temperature (12). Maintenance of body temperature upon acute exposure to cold depletes glycogen in the liver and is a high energy-consuming process (27, 28). Thus, cold exposure challenges the cardiovascular system because of the high demand of energy supply for thermogenesis in BAT and skeletal muscle.

To determine the mechanism(s) underlying cold-induced hypothermia in HF-fed *Pemt*$^{-/-}$ mice, we first explored the possibility of defects in thermogenesis mediated by skeletal muscle and BAT. The thermogenic capacity of skeletal muscle and BAT appeared to be intact in *Pemt*$^{-/-}$ mice fed the HF diet for 2 weeks, because the rates of fatty acid oxidation and expression of mitochondrial electron transport chain proteins in these tissues were not affected by *Pemt* genotype. Although both *Pemt*$^{-/-}$ and *Pemt*$^{+/+}$ mice shivered at the beginning of acute cold exposure, *Pemt*$^{-/-}$ mice showed essentially no shivering after 2 h of cold exposure due to the drop of body temperature. Our data also suggests that the cold-induced hypothermia in HF-fed *Pemt*$^{-/-}$ mice is unlikely caused by an impaired capacity of thermogenesis in BAT or an inability to mobilize fatty acids from the WAT. The data also suggest that mechanisms other than fatty acid catabolism might cause this unsustainable shivering.

BAT is highly vascularized (29), and cold exposure increases cardiac output and promotes blood flow to BAT (23). We found that systolic blood pressure was higher in HF-fed *Pemt*$^{-/-}$ mice than in HF-fed *Pemt*$^{+/+}$ mice (Fig. 5A), consistent with the observation that hypertensive patients are often sensitive to cold (30). However, it is unlikely that the higher blood pressure in HF-fed *Pemt*$^{-/-}$ mice accounts for the hypothermia because blood pressure was not decreased by choline supplementation (Fig. 7F). Moreover, choline elevated blood pressure in *Pemt*$^{+/+}$ mice (Fig. 7F). However, our data do not completely exclude a possible defect in the cardiovascular systems of HF-fed *Pemt*$^{-/-}$ mice and a potential connection with cold-induced hypothermia in these mice. On one hand, increased heat loss due to defective peripheral vessel constriction has been linked to cold-sensitivity in thyroid hormone receptor α1 mutant mice (31). On the other hand, HF-fed *Pemt*$^{-/-}$ mice have choline deficiency (unpublished observations), which might reduce acetylcholine (32), a well-known vascular dilator (33).

BAT consumes not only fatty acids but also large amounts of glucose from blood (34, 35). Cold exposure profoundly increases (by 95-fold) glucose uptake by BAT in rats (36). Chronic infusion of norepinephrine into rats via subcutaneously implanted mini-pumps also markedly increases (by ~50-fold) glucose uptake by BAT (37). Moreover, mice with transplanted BAT have lower body weight, improved glucose tolerance, and increased insulin sensitivity than mice without BAT transplantation, providing strong support for a fundamental role of BAT in global glucose homeostasis (38). In addition, in humans, glucose uptake by BAT is reported to be temperature-sensitive (39, 40), and cold exposure of humans stimulates glucose uptake by BAT (41). Recent studies demonstrate that BAT in humans plays a physiologically significant role in whole-body glucose homeostasis, insulin sensitivity, and energy expenditure (42, 43).

Levels of plasma fatty acids and TG in HF-fed *Pemt*$^{-/-}$ mice were comparable to those in HF-fed *Pemt*$^{+/+}$ mice (Fig. 8B, C), indicating that *Pemt*$^{-/-}$ mice have an intact capability for mobilization of energy storage and fat supply for thermogenesis. However, the 49% lower level of plasma glucose in *Pemt*$^{-/-}$ mice compared with *Pemt*$^{+/+}$ mice (Fig. 9A) might explain why *Pemt*$^{-/-}$ mice are hypothermic. When dietary choline supplementation completely reversed the hypothermia in *Pemt*$^{-/-}$ mice (Fig. 7A), the hypoglycemia and the lower amounts of PEPCK and PGC1α in the livers of *Pemt*$^{-/-}$ mice were restored and increased respectively (Fig. 9B). These observations are consistent with the finding that PEMT deficiency impairs hepatic gluconeogenesis and reduces hepatic glycogen stores and plasma glucose (10, 26). Choline supplementation increases hepatic gluconeogenesis, plasma glucose, and hepatic glycogen in HF-fed *Pemt*$^{-/-}$ mice (26). Interestingly, choline supplementation also increases the lower TG content of BAT in HF-fed *Pemt*$^{-/-}$ mice (supplementary Fig. 4), perhaps reflecting an increased supply of glucose for lipogenesis in the BAT. We conclude, therefore, that compromised hepatic gluconeogenesis and diminished glycogen stores reduce plasma glucose in HF-fed *Pemt*$^{-/-}$ mice leading to an insufficient supply of energy for thermogenesis upon cold exposure.

In summary, HF-fed *Pemt*$^{-/-}$ mice become hypothermic upon cold exposure, which is not due to defective thermogenic capacity of skeletal muscle or BAT, or cold stimulated adrenergic signaling. Choline supplementation prevents the hypothermia and plasma hypoglycemia, highlighting the significant contribution of glucose as an energy substrate for thermogenesis during acute cold exposure in HF-fed *Pemt*$^{-/-}$ mice.

The authors thank Dr. Gary D. Lopaschuk (University of Alberta) for help with interpretation of cardiac function. They thank Dr. Jerome Yager's lab (University of Alberta) for technical help with rectal temperature measurements, and Dr. Guergana Tasseva for help with fatty acid oxidation measurements. They thank Susanne Lingrell and Randal Nelson for excellent technical assistance.

REFERENCES

1. Vance, D. E. 2014. Phospholipid methylation in mammals: from biochemistry to physiological function. *Biochim. Biophys. Acta.* **1838:** 1477–1487.
2. DeLong, C. J., Y. J. Shen, M. J. Thomas, and Z. Cui. 1999. Molecular distinction of phosphatidylcholine synthesis between the CDP-choline pathway and phosphatidylethanolamine methylation pathway. *J. Biol. Chem.* **274:** 29683–29688.
3. Reo, N. V., M. Adinehzadeh, and B. D. Foy. 2002. Kinetic analyses of liver phosphatidylcholine and phosphatidylethanolamine biosynthesis using (13)C NMR spectroscopy. *Biochim. Biophys. Acta.* **1580:** 171–188.

4. Li, Z., L. B. Agellon, T. M. Allen, M. Umeda, L. Jewell, A. Mason, and D. E. Vance. 2006. The ratio of phosphatidylcholine to phosphatidylethanolamine influences membrane integrity and steatohepatitis. *Cell Metab.* **3:** 321–331.
5. Jacobs, R. L., C. Devlin, I. Tabas, and D. E. Vance. 2004. Targeted deletion of hepatic CTP:phosphocholine cytidylyltransferase alpha in mice decreases plasma high density and very low density lipoproteins. *J. Biol. Chem.* **279:** 47402–47410.
6. Noga, A. A., and D. E. Vance. 2003. A gender-specific role for phosphatidylethanolamine N-methyltransferase-derived phosphatidylcholine in the regulation of plasma high density and very low density lipoproteins in mice. *J. Biol. Chem.* **278:** 21851–21859.
7. Yao, Z. M., and D. E. Vance. 1988. The active synthesis of phosphatidylcholine is required for very low density lipoprotein secretion from rat hepatocytes. *J. Biol. Chem.* **263:** 2998–3004.
8. Niebergall, L. J., R. L. Jacobs, T. Chaba, and D. E. Vance. 2011. Phosphatidylcholine protects against steatosis in mice but not nonalcoholic steatohepatitis. *Biochim. Biophys. Acta.* **1811:** 1177–1185.
9. Jacobs, R. L., Y. Zhao, D. P. Koonen, T. Sletten, B. Su, S. Lingrell, G. Cao, D. A. Peake, M. S. Kuo, S. D. Proctor, et al. 2010. Impaired de novo choline synthesis explains why phosphatidylethanolamine N-methyltransferase-deficient mice are protected from diet-induced obesity. *J. Biol. Chem.* **285:** 22403–22413.
10. Ling, J., T. Chaba, L. F. Zhu, R. L. Jacobs, and D. E. Vance. 2012. Hepatic ratio of phosphatidylcholine to phosphatidylethanolamine predicts survival after partial hepatectomy in mice. *Hepatology.* **55:** 1094–1102.
11. Gao, X., J. N. van der Veen, M. Hermansson, M. Ordonez, A. Gomez-Munoz, D. E. Vance, and R. L. Jacobs. 2015. Decreased lipogenesis in white adipose tissue contributes to the resistance to high fat diet-induced obesity in phosphatidylethanolamine N-methyltransferase deficient mice. *Biochim. Biophys. Acta.* **1851:** 152–162.
12. Cannon, B., and J. Nedergaard. 2011. Nonshivering thermogenesis and its adequate measurement in metabolic studies. *J. Exp. Biol.* **214:** 242–253.
13. Vergnes, L., R. Chin, S. G. Young, and K. Reue. 2011. Heart-type fatty acid-binding protein is essential for efficient brown adipose tissue fatty acid oxidation and cold tolerance. *J. Biol. Chem.* **286:** 380–390.
14. Wang, H., M. Yu, M. Ochani, C. A. Amella, M. Tanovic, S. Susarla, J. H. Li, H. Yang, L. Ulloa, Y. Al-Abed, et al. 2003. Nicotinic acetylcholine receptor alpha7 subunit is an essential regulator of inflammation. *Nature.* **421:** 384–388.
15. Jacobs, R. L., S. Lingrell, Y. Zhao, G. A. Francis, and D. E. Vance. 2008. Hepatic CTP:phosphocholine cytidylyltransferase-alpha is a critical predictor of plasma high density lipoprotein and very low density lipoprotein. *J. Biol. Chem.* **283:** 2147–2155.
16. Hirschey, M. D., T. Shimazu, E. Goetzman, E. Jing, B. Schwer, D. B. Lombard, C. A. Grueter, C. Harris, S. Biddinger, O. R. Ilkayeva, et al. 2010. SIRT3 regulates mitochondrial fatty-acid oxidation by reversible enzyme deacetylation. *Nature.* **464:** 121–125.
17. van der Veen, J. N., S. Lingrell, R. P. da Silva, R. L. Jacobs, and D. E. Vance. 2014. The concentration of phosphatidylethanolamine in mitochondria can modulate ATP production and glucose metabolism in mice. *Diabetes.* **63:** 2620–2630.
18. Odenbach, J., X. Wang, S. Cooper, F. L. Chow, T. Oka, G. Lopaschuk, Z. Kassiri, and C. Fernandez-Patron. 2011. MMP-2 mediates angiotensin II-induced hypertension under the transcriptional control of MMP-7 and TACE. *Hypertension.* **57:** 123–130.
19. Cole, L. K., V. W. Dolinsky, J. R. Dyck, and D. E. Vance. 2011. Impaired phosphatidylcholine biosynthesis reduces atherosclerosis and prevents lipotoxic cardiac dysfunction in ApoE-/- mice. *Circ. Res.* **108:** 686–694.
20. Liang, H., and W. F. Ward. 2006. PGC-1alpha: a key regulator of energy metabolism. *Adv. Physiol. Educ.* **30:** 145–151.
21. Cannon, B., and J. Nedergaard. 2004. Brown adipose tissue: function and physiological significance. *Physiol. Rev.* **84:** 277–359.
22. Zechner, R., P. C. Kienesberger, G. Haemmerle, R. Zimmermann, and A. Lass. 2009. Adipose triglyceride lipase and the lipolytic catabolism of cellular fat stores. *J. Lipid Res.* **50:** 3–21.
23. Jansky, L., and J. S. Hart. 1968. Cardiac output and organ blood flow in warm- and cold-acclimated rats exposed to cold. *Can. J. Physiol. Pharmacol.* **46:** 653–659.
24. Alexander, G., A. W. Bell, and J. R. Hales. 1973. Effects of cold exposure on tissue blood flow in the new-born lamb. *J. Physiol.* **234:** 65–77.
25. Wahren, J., and K. Ekberg. 2007. Splanchnic regulation of glucose production. *Annu. Rev. Nutr.* **27:** 329–345.
26. Wu, G., L. Zhang, T. Li, A. Zuniga, G. D. Lopaschuk, L. Li, R. L. Jacobs, and D. E. Vance. 2013. Choline supplementation promotes hepatic insulin resistance in phosphatidylethanolamine N-methyltransferase-deficient mice via increased glucagon action. *J. Biol. Chem.* **288:** 837–847.
27. Barnett, S. A., E. M. Coleman, and B. M. Manly. 1960. Mortality, growth and liver glycogen in young mice exposed to cold. *Q. J. Exp. Physiol. Cogn. Med. Sci.* **45:** 40–49.
28. Meneghini, A., C. Ferreira, L. C. Abreu, V. E. Valenti, M. Ferreira, F. C. Filho, and N. Murad. 2009. Memantine prevents cardiomyocytes nuclear size reduction in the left ventricle of rats exposed to cold stress. *Clinics (Sao Paulo).* **64:** 921–926.
29. Peirce, V., S. Carobbio, and A. Vidal-Puig. 2014. The different shades of fat. *Nature.* **510:** 76–83.
30. Figueroa, J. J., J. R. Basford, and P. A. Low. 2010. Preventing and treating orthostatic hypotension: As easy as A, B, C. *Cleve. Clin. J. Med.* **77:** 298–306.
31. Warner, A., A. Rahman, P. Solsjo, K. Gottschling, B. Davis, B. Vennstrom, A. Arner, and J. Mittag. 2013. Inappropriate heat dissipation ignites brown fat thermogenesis in mice with a mutant thyroid hormone receptor alpha1. *Proc. Natl. Acad. Sci. USA.* **110:** 16241–16246.
32. Gao, X., J. N. van der Veen, L. Zhu, T. Chaba, M. Ordonez, S. Lingrell, D. P. Koonen, J. R. Dyck, A. Gomez-Munoz, D. E. Vance, et al. 2015. Vagus nerve contributes to the development of steatohepatitis and obesity in phosphatidylethanolamine N-methyltransferase deficient mice. *J. Hepatol.* **62:** 913–920.
33. Furchgott, R. F., and J. V. Zawadzki. 1980. The obligatory role of endothelial cells in the relaxation of arterial smooth muscle by acetylcholine. *Nature.* **288:** 373–376.
34. Townsend, K. L., and Y. H. Tseng. 2014. Brown fat fuel utilization and thermogenesis. *Trends Endocrinol. Metab.* **25:** 168–177.
35. Peirce, V., and A. Vidal-Puig. 2013. Regulation of glucose homoeostasis by brown adipose tissue. *Lancet Diabetes Endocrinol.* **1:** 353–360.
36. Shibata, H., F. Perusse, A. Vallerand, and L. J. Bukowiecki. 1989. Cold exposure reverses inhibitory effects of fasting on peripheral glucose uptake in rats. *Am. J. Physiol.* **257:** R96–R101.
37. Liu, X., F. Perusse, and L. J. Bukowiecki. 1994. Chronic norepinephrine infusion stimulates glucose uptake in white and brown adipose tissues. *Am. J. Physiol.* **266:** R914–R920.
38. Stanford, K. I., R. J. Middelbeek, K. L. Townsend, D. An, E. B. Nygaard, K. M. Hitchcox, K. R. Markan, K. Nakano, M. F. Hirshman, Y. H. Tseng, et al. 2013. Brown adipose tissue regulates glucose homeostasis and insulin sensitivity. *J. Clin. Invest.* **123:** 215–223.
39. Ouellet, V., A. Routhier-Labadie, W. Bellemare, L. Lakhal-Chaieb, E. Turcotte, A. C. Carpentier, and D. Richard. 2011. Outdoor temperature, age, sex, body mass index, and diabetic status determine the prevalence, mass, and glucose-uptake activity of 18F-FDG-detected BAT in humans. *J. Clin. Endocrinol. Metab.* **96:** 192–199.
40. Persichetti, A., R. Sciuto, S. Rea, S. Basciani, C. Lubrano, S. Mariani, S. Ulisse, I. Nofroni, C. L. Maini, and L. Gnessi. 2013. Prevalence, mass, and glucose-uptake activity of (1)(8)F-FDG-detected brown adipose tissue in humans living in a temperate zone of Italy. *PLoS One.* **8:** e63391.
41. Orava, J., P. Nuutila, M. E. Lidell, V. Oikonen, T. Noponen, T. Viljanen, M. Scheinin, M. Taittonen, T. Niemi, S. Enerback, et al. 2011. Different metabolic responses of human brown adipose tissue to activation by cold and insulin. *Cell Metab.* **14:** 272–279.
42. Chondronikola, M., E. Volpi, E. Borsheim, C. Porter, P. Annamalai, S. Enerback, M. E. Lidell, M. K. Saraf, S. M. Labbe, N. M. Hurren, et al. 2014. Brown adipose tissue improves whole-body glucose homeostasis and insulin sensitivity in humans. *Diabetes.* **63:** 4089–4099.
43. Matsushita, M., T. Yoneshiro, S. Aita, T. Kameya, H. Sugie, and M. Saito. 2014. Impact of brown adipose tissue on body fatness and glucose metabolism in healthy humans. *Int. J. Obes. (Lond).* **38:** 812–817.